A Novel Transceiver Model for Polar Transform Optical (PTO-) OFDM for Visible Light Communication (VLC) Based on Peak to Average Power Ratio Reduction using Precoding

Oumar Sacko, Stephen Musyoki, Vitalice K. Oduol

Abstract: ***Indoor visible light communication (VLC) has the potential of providing high data rates for short-range wireless communication with a relative spatial elevated security in contrast to a radiofrequency wireless one. To support that high data stream, Orthogonal Frequency Division Multiplexing (OFDM) is used; however, due to the limited operational bandwidth of the commercial white light-emitting diode (LED), signal processing techniques are used to increase the efficiency of the OFDM and to adapt OFDM to VLC systems. As a major concern, the intensity modulation direct detection necessary for VLC requires positive real signal, this is dealt with by imposing Hermitian pre-possessing or Cartesian to polar conversion post-processing to the OFDM. The use of the Cartesian to polar converter allows the transmission of complex OFDM symbols through the intensity modulation channel. A polar transform optical (PTO-) OFDM presented here as an improvement and simplification of previous polar optical OFDM schemes gives an efficient transceiver architecture. Nevertheless, both OFDM transmission techniques for Visible optical links, similar to radiofrequency (RF), suffer greatly from irregular excessive Peak-to-Average power ratio (PAPR). Higher PAPR reduces the power efficiency of the On-Off Keying (OOK) based on pulse amplitude modulation (PAM). Furthermore, it also is recommendable to reduce the PAPR for conformity with eye safety. A precoding technique is proposed to reduce the PAPR of intensity-modulated for direct detectability of the OFDM signal destined for the wireless optical link using Cartesian-to-Polar conversion. Based on the enhanced processing at the front ends and using MATLAB simulation, it is proven that the presented model can improve the link parameters including the bit error rate (BER) and signal to noise ratio (SNR) and bandwidth efficient compared to Hermitian modified ones.***

Keywords**:** ***Intensity modulation Direct detection, PAPR precoding, Polar Transform Optical OFDM, Pulse Coded Modulation, Visible light communication.***

I. INTRODUCTION

The ever-increasing demand for high rate reliable exchange of information in an overwhelmingly congested RF spectrum has led to the exploration and exploitation of higher spectrum in visible light.

As a new paradigm of wireless communication enjoying enormous unlicensed frequency band, VLC uses LED and photodetector (PD) to establish reliable data transmission while its illumination functions are maintained [1]. LED as transmission front end has many attractive attributes including low power consumption, cost-effectiveness, free from electromagnetic interference and intrinsic spatial security [2], [3]. Despite those many attractive benefits, the usage of LEDs poses challenges in the design of the transceiver of VLC system. The modulation bandwidth of the off-the-shelf LEDs is mildly narrow, as a result, the bit error rate (BER) of the link deteriorates due to inter-symbol interference (ISI) if a high-frequency signal is used at an elevated transmission rate. OFDM is well known to be effective against narrowness and ISI in frequency bandwidth by flattening the channel into multiple parallel lower speed streams [4]. Nonetheless, the constrained nature of the VLC channel requires transceiver to use simplified transmission and reception. Intensity modulation and direct detection permit an inexpensive exchange of information-bearing signals between LED and photodetector.

Complex modulation signals including multiple quadrature amplitude modulation (M-QAM) and quadrature phase-shift keying (QPSK) combined with OFDM for link efficiency go through adaptive adjustment before applying IM, which reduces its established performance. Many studies have presented different methods of modification to meet the real and positive unipolar signal not only at the cost of frequency efficiency but also signal power. The separate transmission of magnitude and phase of OFDM signal known as polar OFDM [5] shows many potentials since it eliminates the need for a Hermitian symmetry operation, and, the link performance can be improved by using coded pulse amplitude modulation (PAM) transmission of the phase [5], [6]. The polar and magnitude-phase OFDM models require no Hermitian transform operation before the IFFT process. By coding the phase using PAM before analog-digital converter (ADC), an attempt was made to remedy the link deterioration due to the angle noise, while using clipping to control the PAPR [3]. Arguably, a significant disadvantage of the use of OFDM arises from the high PAPR, a large swinging range for signal amplitude particularly as the high-frequency carriers and baseband constellation increase in size [7], [8].

Revised Manuscript Received on August 05, 2020.

***** Correspondence Author

Oumar Sacko*, Telecommunication Program, Pan African University Institute for Basic Sciences Technology, and Innovation (PAUISTI), Jomo Kenyatta University of Agriculture and Technology (JKUAT), Nairobi, Kenya. E-mail: oumar.sacko@student.jkuat.ac

Stephen Musyoki, Dept. of Telecommunication and Information Engineering of organization, The Technical University of Kenya (TUK), Nairobi, Kenya. E-mail: smusyoki@yahoo.com

Vitalice K. Oduol, Dept. of Electrical & Information Engineering, University of Nairobi (UoN), Nairobi, Kenya. E-mail: vitalice.oduol@gmail.com

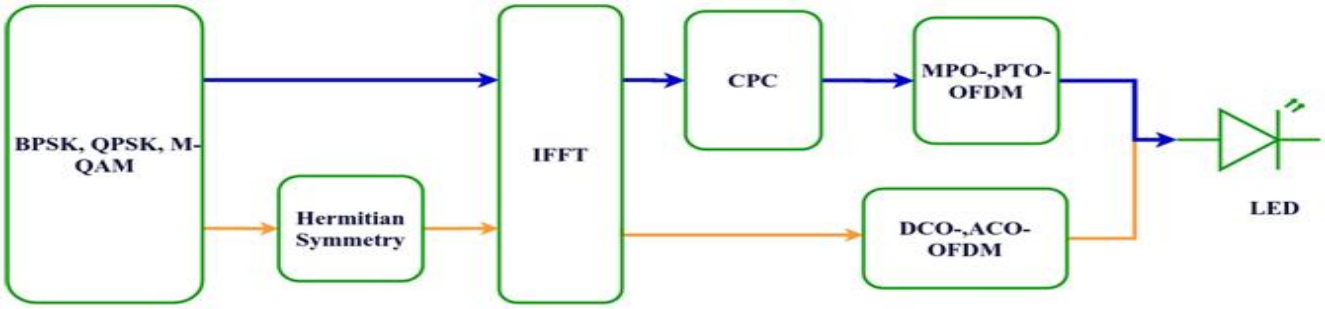

Fig. 1. OFDM adaptations in a VLC modular comparison

High PAPR causes nonlinear distortion in power amplifiers in RF systems, in the same way, it results in similar effects in optical transmission. The limited dynamic range (DR) of LED restricts the maximum tolerable signal amplitude beyond which the diode will be forced to operates in its non-linear region causing growth in both output back-off (OBO) or input back-off (IBO)[9]. The growth of the back-off ratio gives rise to power spillage and inband spectral distortion noise consequently a penalty in transmit power wastage is bound to happen [10]. The combination of nonlinear distortion noise and elevated PAPR deteriorate considerably the BER of OFDM system in VLC. Different techniques based on clipping and pulse shaping have been presented in the literature to remedy the issues related to PAPR. Clipping which simply forces the LED to remain in its linear region by keeping the transmit amplitude below a predefined level costs in the reduced power efficiency of the system [8] [10].

Precoding and scrambling techniques have also been presented exploiting diverse properties of the signals and processing techniques to keep the signal power controlled by the means of increasing the average power, subcarrier count, spreading the signal constellation or adding side information. The benefits of a PAPR reduction technique adapted from RF system include a pronounced improvement in optical link reliability in the case of Hermitian symmetry-based OFDM such as DCO-, ACO-OFDM, and their variants. Moreover, for Cartesian-to-Polar conversion (CPC) OFDMs and magnitude phase (MP)-OFDM, the reduction performance is identical for RF and VLC system. Since the signal would pass through similar processing until the entry of CPC function as in Fig. 1. Likewise, the same parameters tuning is applicable.

The rest of the paper is organized as follows: the next, section II deals with a brief literature review of different PAPR reduction techniques, then the precoded Polar based OFDM principle is discussed in section III. The simulation results and conclusion are presented respectively in section IV and V.

II. LITERATURE REVIEW

The main techniques reported in the literature which are utilized to control the disproportionate outgrowth of the PAPR fall broadly under companding, clipping, scrambling, pulse shaping or precoding. Bearing with them different advantages and drawbacks in relation to the communication system complexity as well as resource consumption.

A. Companding

First all, nonlinear companding is based on the treatment of OFDM signal like speech signals, thereby applying compressing method such as μ-law [11], such process would cause a considerable magnification in symbols with small amplitude and scale down of high magnitude symbol resulting in an amplification of the overall average power. For a given peak power, an increase in the average OFDM frame power conduces to lowering the PAPR. However, a raised average power requires an augmentation in the transmission power of the system. To address such issues another nonlinear companding technique based on exponential transform was presented in [4]. It tries to keep the average power constant while reducing the PAPR. Compared to former μ-law, the reported PAPR and BER are improved. Similar to the results in [11], the growth of the outbound power level remains stable for simpler mapping method i.e. BPSK and QPSK; even though for advanced baseband M-QAM constellation ($M \geq 32$) further analysis is indispensable. Triangular companding in [11], as an improvement of trapezium distribution based companding [12], reduces both the complexity of the latter companding operation as well as maintains a fair level of

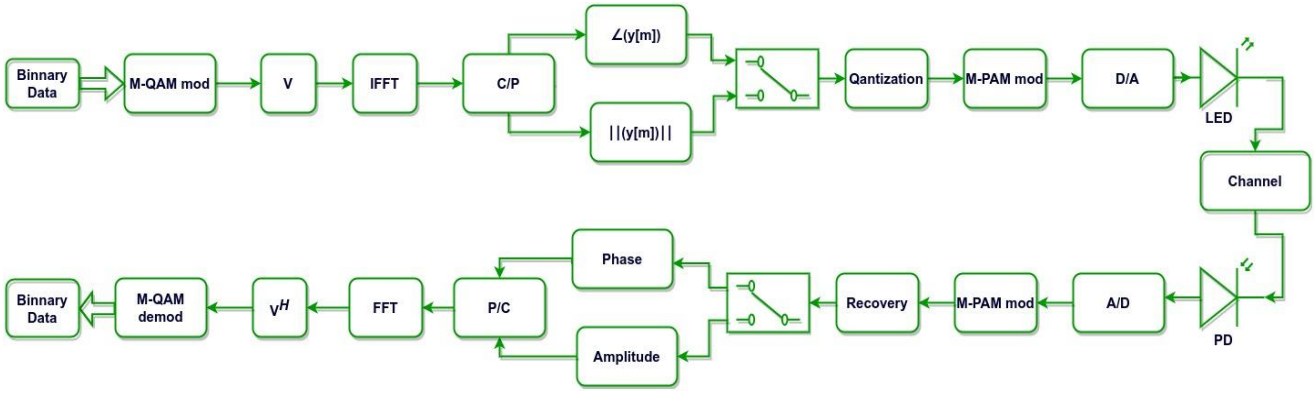

Fig. 2. PTO-OFDM

Polar transform-based M-PAM OFDM transceiver architecture showing the processing stage and submodules system performance as the diverse parameters controlling the distribution profile are tuned.

B. Clipping and Pulse Shaping

As PAPR reduction technique clipping has been explored in [6], [12]–[14]. It is easy to apply since it performs solely thresholding to the outliner amplitude levels leaving others unaffected [9]. It reported in [12] that the PAPR reduction incurred by clipping is offset by the spectral regrowth and the ICI it induces, quantifiable in terms of IBO/OBO. Iterative filtering and clipping can partly curb the spectral regrowth by containing the spectrum of the signal. However, it necessitates replicating the IDFT operation for each iteration [13]. Such a solution raised the complexity and cost of transceivers. Because the reduction performance is directly related to the number of iterations i.e. number of IDFT and filtering submodule and operation thus it becomes computationally expensive to achieve the desired outcome. Pulse shaping can also be used in the time domain to limit the PAPR of the OFDM signal. It removes the need for extra filtering with repetitive IFFT operates; besides, there is no need for the transmission of side information [8]. By introducing a bit of correlation between the OFDM symbol in a frame, the PAPR shrinks. However, a modification in OFDM signal shape requires the use of a special detector at received since orthogonality does not hold anymore between symbols for ease of detection. In [15], a time-domain infinite impulse response (IIR) prototype filter is applied while maintaining the orthogonality; however, compromise is necessary to design an optimal truncated bin count. The PAPR lowering performance is directly related to the ratio of the truncated IIR size and OFDM carrier count. Therefore, as the subcarrier increases, a longer bin size must be employed.

C. Scrambling

Selected mapping introduced in [16] is another mechanism for PAPR minimization which belongs to a class of technique classified in [9] as scrambling. Fundamentally, the lowest PAPR statistics time-domain frame is chosen from multiple copies of possible OFDM modulated signals. The decoding of that transmitted frame is carried out with the help of side information (SI). The sensitivity of the system with SI detection probability error determines the reliability of the link, in addition to the bandwidth that it occupies while carrying no usable information data. The reliance on SI has been eliminated in [16]; still, the reduction of the PAPR relies on an elevated disproportion between subcarriers size and baseband constellation nature. Consequently, it is only suited for PSK or M-QAM with $M \leq 16$ as the presumption of the individual OFDM symbol power being interchangeable with an average energy of the frame does not hold for QAM constellation of size $M \geq 32$. The tone reservation technique repartitions the sub-carriers into two sets where one carries the data signal. The non-carrying frequencies are used as peak reduction tone (PRT) carriers. It offers similar results for both OFDMA and direct sequence code division multiple access (DS-CDMA) [17]. A modification is presented in [18], where the insertion of dummy random Gaussian (IDRG) carriers replaces PRT, based on the scheme of partial transmit sequence (PTS). Nonetheless, it reduces the amount iteration to half of the normal PTS while keeping PAPR low at the proportion of inserted carrier size. Hence, it consumes transmission power and bandwidth. On the other hand, Tone Injection (TI) does not reserve any carrier for other than data transmission, TI supports an expanded QAM constellation at the cost of more transmission power in addition to the tremendous computational load at transceivers.

D. Precoding

Precoding is also a promising PAPR controlling strategy that applies a predefined small PAPR sequence (code) to the baseband PSK or QAM modulated signal in advance of OFDM operation. Hence, it optimizes the constellation statistics leading to a lower time-domain OFDM swing [19], [20]. Zadoff Chu sequence known for its efficiency against PAPR has been adopted as part of the 3G/4G standard [21]. In [1], an extended Zadoff-Chu sequence used to form a Zadoff-Chu matrix (ZCM) was utilized to preprocess the VLC link for the case of DC biased OFDM. It also supports a stable SNR over a range of different biasing values critical for the power inefficiency of DC-OFDM. The computational complexity is related to the complex-valued Zadoff Chu sequence length which is the square of the subcarrier number. Similarly, the precoding used in [19] exerts on RF link. The precoding matrices keep the orthogonality among OFDM subcarriers, as a result, the error performance is conserved. This paper adapts the latter approach to optical wireless links with a novel transceiver design enabled by the resultant reduced PAPR.

E. Factors Influenced by OFDM's PAPR

A limiting factor to any OFDM systems, including RF wireless or optical wireless, the significance of PAPR comes into effect at the point of amplification and conversion into an analog signal the time domain digital i.e. DFT signal. The DAC and ADC operations take place at the front ends nearby propagation modules. While the power amplifier (PA) is used in combination with other submodules in RF systems, the VLC mainly depends on a simpler interface joining PA with LED as the signal propagator. The signal to quantization noise ratio (SQNR) of the DAC decreases leading to declining the power efficiency of the LED and photodetector (PD) in VLC systems. The linear operation of the LED has to maintained despite its limited dynamic range to reduce backoffs and out-of-band radiation [9], giving rise to an interest of exploring strategies to counter the random overshoots in the time domain transmit signal.

III. POLAR TRANSFORM BASED OFDM TRANSMISSION PRINCIPLE FOR VLC

Diverse modulation schemes must be combined on different layers of the transceiver to achieve strong link capacity. To overcome different link shortcoming including power and bandwidth efficiency, QAM, OFDM, and PAM modulation techniques come together to set up a reliable channel. Since VLC, transmits only the real and positive signal, it is not straight forward to send any complex modulation scheme signal that includes QAM and OFDM; unless it goes through adaptation processes. Hermitian based OFDM seeks to suppress either the imaginary or real components of the complex modulated signal. The resulting signal takes both positive and negative scalar values that make it necessary either the use of a DC biased (DC-OFDM) as an offset that the final signal to be transmitted is forced to be above. Another way would be to asymmetrically clipping off the negative values (ACO-OFDM) and transmitting the remaining positive values without the need for a DC biasing. The former suffers from power inefficiency on account of the non-carrying DC, while the latter endures bandwidth inefficiency due to clipping half of the carriers.

On the other hand, the polar transform-based (PT-) OFDM is identical to RF OFDM except after (before) IFFT (FFT) operation on the transmitter (receiver). The IFFT process is followed by a Cartesian to polar converter so that the complex signals become transmissible as phase and norm over the scalar channel. The polar representation of OFDM frame over PAM modulation becomes more resistant to the ICI [6]. However, for power constraint and ADC resolution limitations, PAPR reduction is applied to improve the power efficiency of the link.

A. PAPR Reduction Using Precoding

For a given baseband signal such as M-PSK or M-QAM signal $\boldsymbol{X} = [X_o, X_1, \dots, X_{N-1}$, the precoded version $Y_q, q \in \{0,1,2, \dots, Q-1\}$ is obtained as follows,

$$\boldsymbol{Y} = \boldsymbol{VX} \tag{1}$$

Where $\boldsymbol{V} = \left[\boldsymbol{v_0}, \boldsymbol{v_1}, \dots, \boldsymbol{V_{Q-1}}\right]^{\boldsymbol{T}} \in \mathbb{C}^{Q \times N}$ is the precoding matrix. Its raw size $Q = N + N_p \; with \;\; N_p = \mathfrak{n} \times N$, as in [19], in contrast to that of [1], it is a non-square matrix where $Q(\geq N)$ represents the number carrier utilized in IFFT and N actual number of M-QAM in the OFDM frame. Therefore, the price of that technique is in the form of the amount of Nv sub-carriers. The resultant signal is modulated with IDFT matrix $\mathcal{F}_m^{\mathcal{H}}, m = \{0, \dots, Q-1\}$,

$$\begin{aligned} y[m] &= \mathcal{F}_m^{\mathcal{H}}\mathbf{Y} \\ &= \mathcal{F}_m^{\mathcal{H}}\mathbf{VX} \\ &= \frac{1}{\sqrt{Q}}\sum_{q=0}^{Q-1} Y_q \exp\left(\jmath\frac{2\pi}{Q}mq\right) \\ &= \frac{1}{\sqrt{Q}}\sum_{q=0}^{Q-1}\sum_{n=0}^{N-1} v_{qn}\, X_n \exp\left(\jmath\frac{2\pi}{Q}mq\right) \end{aligned} \tag{2}$$

A modified version of MP-OFDM is considered, instead of just transmitting M-PAM coded of the phase, both norm and phase components of the polar transformed OFDM signal are processed in an identical manner before transmission in successive frames. They both go through quantization before M-PAM modulation since the dynamic range of the magnitude component is significantly by precoding.

$$y[m] = r_m \exp(\jmath\theta_m) \Leftrightarrow \begin{cases} r_m = abs(y[m]) \\ \theta_m = arg(y[m]) \end{cases} \tag{3}$$

The pre-processor matrix $\boldsymbol{V}$ is designed such that the raw size Q of the precoder, and by extension, the number of subcarriers frequencies is chosen to satisfy the lessening sought after for the maximum desired peak power of the amplifier. The parameter $N_p > 0$ induces a scaling down effect on the time domain IFFT power by flattening and spreading the signal energy. Successively, the magnitudes and the phases are transmitted in different frames for an equal amount of time slot. Consequently, they experience the additive noise of the channel, in addition to the quantization noise from the transmitter PAM process.

The entries of the precoding matrix are chosen as in [19], i.e. $v_{q,n} = v_{q,0}e^{-\jmath 2\pi\frac{qn}{N}}$. The first column $v_{q,0}$ of the precoder is given by (4).

$$v_{q,0} = \begin{cases} \dfrac{(-1)^q}{\sqrt{N}}\sin\left(\dfrac{\pi q}{2N_p}\right), & 0 \leq q < N_p \\ \dfrac{(-1)^q}{\sqrt{N}}, & N_p < q \leq N \\ \dfrac{(-1)^q}{\sqrt{N}}\cos\left[\dfrac{\pi(q-N)}{2N_p}\right], & N \leq q \leq Q-1 \end{cases} \tag{4}$$

B. Statistics of the OFDM signal

According to the central limit theorem [22], $y[m]$ adopts a Gaussian random distribution with zero mean and variance σ_y^2. It is related to the derived QAM constellation energy σ_x^2 as follows.

$$\begin{aligned}\sigma_y^2 &= \mathbb{E}\{|y[m]|^2 - \mu_y^2\} \\ &= \mathbb{E}\left\{|\mathcal{F}_m^{\mathcal{H}}|^2 |v_q|^2 |X[n]|^2\right\} \\ &= \mathbb{E}\{|X[n]|^2\} \\ &= \sigma_x^2\end{aligned} \tag{5}$$

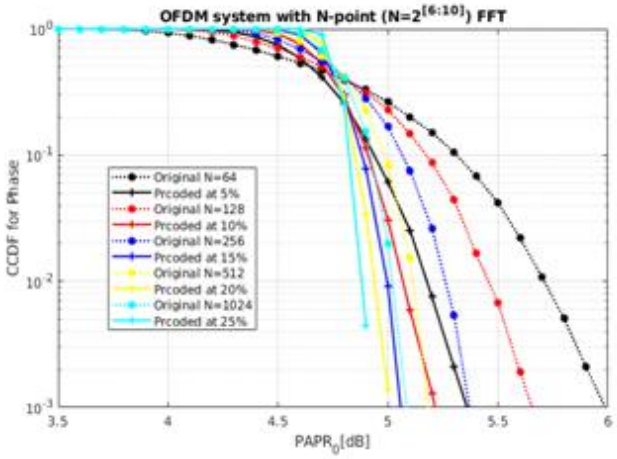

Fig. 3. Phase CCDF profile

Effect of precoding on the phase CCDF distribution, an observable reduction on CCDF between precoded and original signal phase, the reduction improves with the increase in precoding subcarrier ratio ɲ.

The Precoding brings negligible alteration to the initial expectation of the OFDM system. Its effect comes about in flattening the maximum value that the time domain OFDM signal reaches in amplitude and phase also, where its use against that ratio. As they pass through the polar conversion process, the magnitude and phase portions of the signal are characterized by their statistical distribution. its magnitude r_m follows a Rayleigh distribution such that $E\{r_m\} = \sigma_y\sqrt{\frac{\pi}{2}}$, $var[r_m] = \sigma_y^2\frac{4-\pi}{2}$. The inherent characteristic of the phase variation can be modeled without loss of generality in the range $[0, 2\pi)$, and as uniform distribution with mean $E\{\theta_m\} = \pi$ [5].

C. PAPR Reduction

The PAPR impairs the efficiency of the OFDM modulation scheme in linear systems. As the signal passes through the power amplifier and DAC, the high PAPR ends up forcing those submodules of the communication system to exit their designated ranges of operation. A reduced PAPR is required in VLC not only for a better signal to noise plus interference ratio (SINR) but also for the constraints placed on the luminosity of LEDs conforming with regulation such as minimum required office or room illumination. In the case of PAM link, the magnitude of the signal, as well as the phase is of concern. The PAPR in decibel (dB) for an OFDM magnitude frame is given as,

$$\text{PAPR}_{y[m]} = \frac{\max\ |y[m]|^2}{\mathbb{E}\{|y[m]|^2\}} \tag{6}$$

While the impact on the phase of input power affecting the DAC is not a concern in RF and other non-polar VLC OFDM i.e. a linear PA has no effect on the angle components of those schemes. However, because the magnitude and phase are treated identically, they experience a similar degradation throughout the link. However, the distribution of the phase is slightly altered by precoding; and, a reduction in PAPR of $1dB$ at 10^{-3} probability can be achieved using a ratio of 10% of the total OFDM carrier.

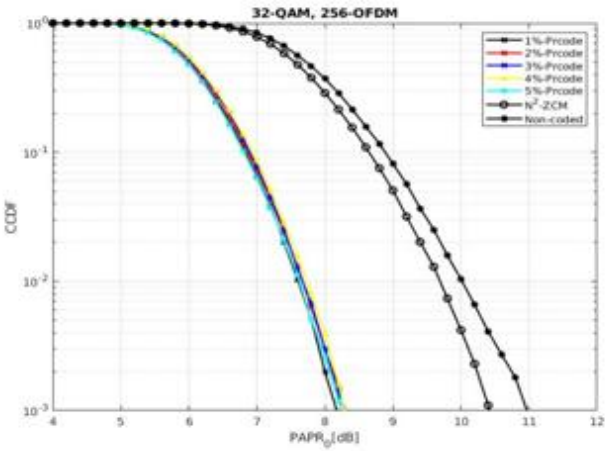

Fig. 4. Amplitude CCDF profile

Performance of PAPR reduction techniques for lower ɲ factor and fixed QAM and OFDM subcarriers.

A noticeable improvement can be seen in the phase distribution profile as ɲ values increase. From Fig. 3 with $ɲ = 5$ a reduction of $0.6dB$ at a CCDF of 10^3 with 64-OFDM. The performance of PAPR reduction techniques are typically presented using the complementary cumulative distribution function (CDF), expressing the probability of PAPR above a desired threshold PAPR_0[dB]. Ideally, 0dB level crossing would be the desired threshold, nevertheless, a higher value is chosen for practical purposes. The maximum reachable power can be found by using oversampling. It is sufficient to oversample at 4-fold to reach the maximum possible power.

$$\text{CCDF}_{y[m]} = \text{Prob}(\text{PAPR}_{y[m]} > \text{PAPR}_0) \tag{7}$$

A satisfactory reduction on the amplitude PAPR can be attained with a value of ɲ as low as 1 percent of the primary N subcarriers as in Fig. 4. With that ratio, as high as $2dB$ reduction from the original modulated signal can be obtained with a probability of 10^{-3}.

D. Recovery of Transmit Signal

To simplify the notation the subscript θ, r are omitted when it does not lead to ambiguity. A perfect synchronization with a channel attenuation of unity is assumed. The recovered polar form signal from the k^{th} M-PAM symbol is written as

$$\begin{aligned} r[k] &= r_m + z_r[k] \\ \theta[k] &= \theta_m + z_\theta[k] \end{aligned} \tag{8}$$

The noise $z_\theta[k]$ and $z_r[k]$ are statistically identical, they are both constituted of quantization noise $z_{qu}[k]$ and additive white Gaussian noise $z_{ga}[k]$, owing to the similarity in their sources. the ambient and background light, the electronic impairments constitute the main noise sources. They are expressed below as,

$$\begin{aligned} z_r[k] &= z_{ga}^{(r)}[k] + z_{qu}^{(r)}[k] \\ z_\theta[k] &= z_{ga}^{(\theta)}[k] + z_{qu}^{(\theta)}[k] \end{aligned} \tag{9}$$

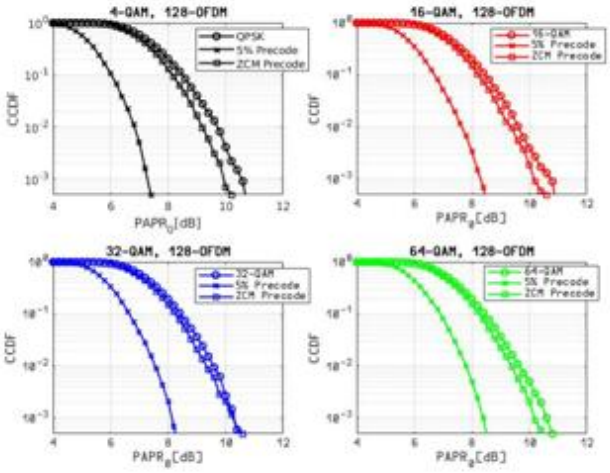

Fig. 5. PAPR reduction performance (1)

with a varying QAM constellation and fixed N_{FFT} for both coding techniques and uncoded OFDM signal are contrasted.

The quantization noise z_{qu} is uniformly distributed, while the additive white noise of variance σ_{ga} is normally distributed for angle and magnitude indicated by superscripts (r), (θ). Precoding allows the use of a simplified transceiver where the same submodules perform phase and amplitude transmit and receipt processing, in contrast to the model of [12]. Since the quantization range differ, the resolution $\lambda = \Delta/2^L$ varies, allowing room for power allocation depending on the angle of amplitude. On the other hand, the additive ones are related to the channel instead of the nature of the transmit signal statistics.

The OFDM signal is reconstructed after the receipt of phase and magnitude information in each frame. for k^{th} subcarrier, $k \in \{0,1,\dots Q\}$, $s[k] = r[k]\exp(\jmath\theta[k])$

$$\begin{aligned} s[k] &= \left(\frac{1}{\sqrt{Q}}\sum_{q=0}^{Q-1} Y_q \exp\left(\jmath\frac{2\pi}{N}kq\right) + z_r[k]\right)\exp(\jmath z_\theta[k]) \\ &= \left(\frac{1}{\sqrt{Q}}\sum_{q=0}^{Q-1}\sum_{n=0}^{N-1} v_{qn}\, X_n \exp\left(\jmath\frac{2\pi}{N}kq\right) + z_r[k]\right)\exp(\jmath z_\theta[k]) \end{aligned} \tag{10}$$

For the baseband M-QAM mapped data, IFFT modulated symbols in the frame $\boldsymbol{s} = \{s[k]\}_{k=0}^{Q}$ is then processed with the transpose of the complex conjugate of the precoding matrix $\mathbf{V}$ after the FFT operator $\mathcal{F}$. Demodulating the OFDM signal $\mathbf{s}$, the QAM signal vector at the user terminal becomes $\mathbf{S} = \mathcal{F}\mathbf{s} = \left[S_0, S_1, \cdots, S_{Q-1}\right]$

$$\begin{aligned} S_p &= \sum_{k=o}^{Q-1} s\,[k]\exp\left(\jmath\frac{-2\pi}{N}kp\right) \\ &= \frac{1}{\sqrt{Q}}\left(\sum_{k=0}^{Q-1}\sum_{q=0}^{Q-1}\sum_{n=0}^{N-1} v_{qn}\, X_n \exp\left(\jmath\frac{2\pi}{N}k(q-p) + \jmath z_\theta[k]\right)\right) + \Omega_p \end{aligned} \tag{11}$$

The factor Ω_p in (11), can be expressed in (12). It combined the distortion resulting from the phase and amplitude component as additive noise.

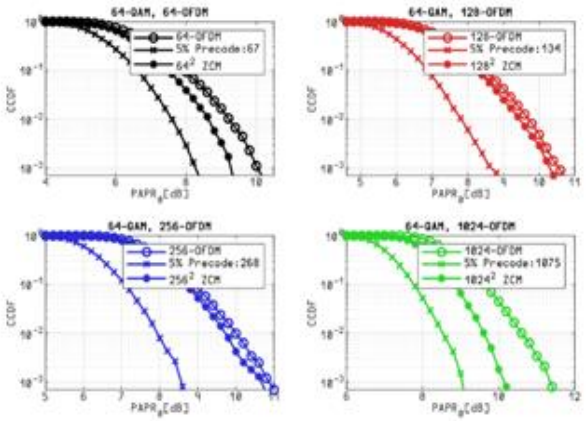

(12)

Fig. 6. PAPR reduction performance (2)

with varying OFDM carrier size for both coding techniques and uncoded OFDM signal are compared.

$$\Omega_p = \sum_{k=0}^{Q-1} z_r\,[k]\exp\left(\jmath\left(z_\theta[k] - \frac{2\pi}{N}kp\right)\right)$$

It obeys a Gaussian distribution with zero mean and standard deviation σ_{Ω_p} formulated in (13) as derived from [6]. The parameter λ stands for the quantization resolution of phase, with L-bits word length. The variation of the range Δ for phase is however small. However, it fluctuates in case of amplitude with different frames.

$$\sigma_{\Omega_p}^2 = \frac{Q\left(\left(\sigma_{ga}^{(r)}\right)^2 + \left(\sigma_{qu}^{(r)}\right)^2\right)\sin(\lambda_\theta)}{\lambda_\theta}\exp\left(-2\left(\sigma_{ga}^{(\theta)}\right)^2\right) \tag{13}$$

The corrupted QAM signal eventually is retrieved after decoding by using the complex conjugate of the transpose precoding matrix $\mathbf{V}^{\mathcal{H}} \in \mathbb{C}^{N\times Q}$, let $\tilde{\mathbf{X}} = [\tilde{X}_0, \tilde{X}_1, \cdots, \tilde{X}_{N-1}]$ denotes the recovered mapped signal. By using (11), in the matrix and vectorial notation, the estimated QAM symbols are extracted by exploiting the orthogonality property of the OFDM and precoding matrices.

$$\begin{aligned} \tilde{\mathbf{X}} &= \mathbf{V}^{\mathcal{H}}\mathcal{F}\mathbf{s} \\ &= \mathbf{V}^{\mathcal{H}}\mathcal{F}\left((\mathcal{F}^{\mathcal{H}}\mathbf{V}\mathbf{X} + \mathbf{z}_r)\boldsymbol{\Theta}\right) \\ &= \mathbf{V}^{\mathcal{H}}\mathcal{F}\boldsymbol{\Theta}\mathcal{F}^{\mathcal{H}}\mathbf{V}\mathbf{X} + \mathbf{V}^{\mathcal{H}}\mathcal{F}\mathbf{z}_r\boldsymbol{\Theta} \\ &= \mathbf{V}^{\mathcal{H}}\boldsymbol{\varpi} + \mathbf{V}^{\mathcal{H}}\Omega_p \end{aligned} \tag{14}$$

Where $\boldsymbol{\Theta} = \exp(\jmath\mathbf{z}_\theta)$, and $\mathbf{z}_\theta = \left[z_0, z_1, \cdots, z_{Q-1}\right]$ the phase noise corrupting the angle component of the PAM signal. Therefore, the w^{th} element of recovered QAM vector is given as $\tilde{X}_w = \boldsymbol{v}_w^*\mathbf{S} = v_w^*\boldsymbol{\varpi} + \boldsymbol{v}_w^*\Omega_p = S_w + \Omega_w$.

Similarly, the factor Ω_w indicating the second term in the above expression is the projection of $\boldsymbol{\Omega_p}$ onto an orthonormal vector space $\mathbf{V}^{\mathcal{H}} \in \mathbb{C}^{Q\times N}$; hence, its variance $\sigma_{\Omega_w}^2$ remains approximately constant.

$$\begin{aligned}\Omega_w &= \sum_{p=0}^{Q-1} v_{wp}^{*} \sum_{k=0}^{Q-1} z_r[k] e^{-\jmath\left(\frac{2\pi}{Q}kp - z_\theta[k]\right)} \\ &= \sum_{p=0}^{Q-1}\sum_{k=0}^{Q-1} v_{0p}\, z_r[k] \exp\left(-\jmath\left(\frac{2\pi}{N}(kp+wp) - z_\theta[k]\right)\right)\end{aligned} \tag{15}$$

Its variance thus is derived from (13), which follows from the fact that $\mathbf{V}^{\mathcal{H}}$ being unitary; therefore, its effect vanishes from the variance.

$$\begin{aligned}\sigma_{\Omega_w}^2 &= \sum_{p=0}^{Q-1} \left| v_{wp}^{*} \right|^2 \mathrm{var}(\Omega_w) \\ &\approx \sigma_{\Omega_\mathrm{p}}\end{aligned} \tag{16}$$

E. Analytical BER Formulation

Analogous to [19], the overall SINR of the demodulated OFDM symbols simplified becomes,

$$\xi = \frac{\sigma_y^2 \mathbb{E}\{|\mathcal{L}(0)|^2\}}{\sigma_y^2 \sum_{i=0}^{N-1} \mathbb{E}\{|\mathcal{L}(i)|^2\} + \sigma_{\Omega_w}^2} \tag{17}$$

Assuming that attenuation is unity, the link behaves in the form of the regular additive noise channel whereby the effects of quantization and the Gaussian noise are lumped together (14). The terms $\mathbb{E}\{|\mathcal{L}(i)|^2\}$, $i \in \{0,1,2,\cdots,Q-1\}$ stands for the scaled inter-symbol interference (ISI) from other carriers of index $i \geq 1$.

An approximation of the analytical BER of the VLC channel is given [7]. However, the simulated performance deviates from the graph of (18).

$$\mathrm{BER} \approx \frac{\sqrt{\mathrm{M_d}}\text{-}1}{\sqrt{\mathrm{M_d}}\log_2\left(\sqrt{\mathrm{M_d}}\right)} \mathrm{erfc}\left(\sqrt{\frac{3\xi}{2(\mathrm{M_d}\text{-}1)}}\right) \tag{18}$$

IV. RESULTS

The effect of the precoding on both the phase and the magnitude is compared with uncoded as well as Zadoff Chu sequence precoding. Software simulation is performed with a range of QAM constellation varying from 8 to 64. A wide range of OFDM subcarrier count is also adopted to have reliable simulation results; so that the outcome on both performances is established. Two set values targeted for ɲ, very low {1 2, 3,4,5} and medium {10, 15, 20, 25}.

From the above set of figures, the PAPR reduction observed in the magnitude transmit power in Fig. 4 is almost thrice that of the scaling down of the phase counterpart seen in Fig. 3. As the QAM constellation increases in size, a slight rise is observed in the maximum reached PAPR over the CCDF range simulated in Fig. 5. It is fixated around $8dB$ for a probability of 10^{-3} achieving about $2dB$ reduction. A similar case is valid also for Fig. 6 likewise, an overall reduction of approximately 2dB at a probability rate of 10^{-3}. While there is a small improvement of PAPR for the case of the ZCM technique seen in both figures.

The BER profiles depict that the effect of the precoding is insignificant. However, compared to the ZCM scheme, a minute improvement is noticed. Remarkable reduction in the BER results from rising the QAM constellation size as depicted in Fig. 7, which stands opposite the negligible change as the precoding percentage ɲ grows Fig. 8 or OFDM subcarrier Fig. 9.

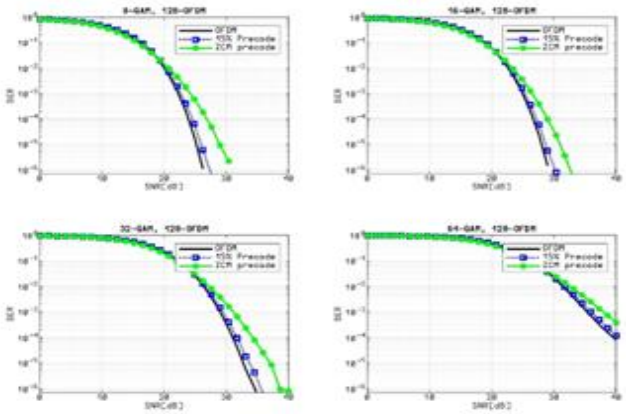

Fig. 7. BER variation with respect to MQAM

By setting fixed size for ɲ=15%, and subcarrier count N_{FFT}=128

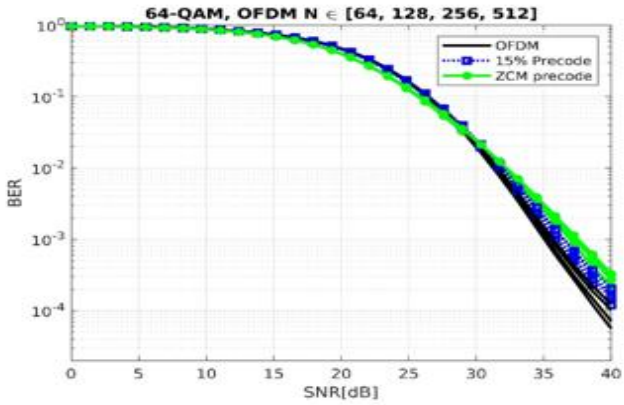

Fig. 8. BER performance for different N_{FFT}

the BER for fixed QAM size and ɲ=15%, in contrast with ZCM precoded and uncoded OFDM

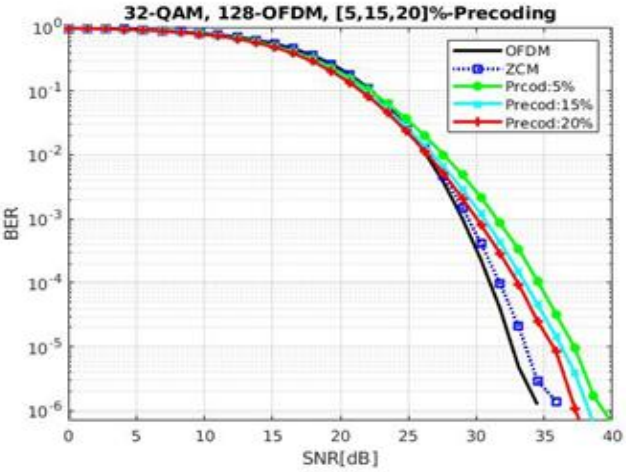

Fig. 9. BER performance for PTO-OFDM

BER for various precoding ratio over fixed subcarrier number and QAM size

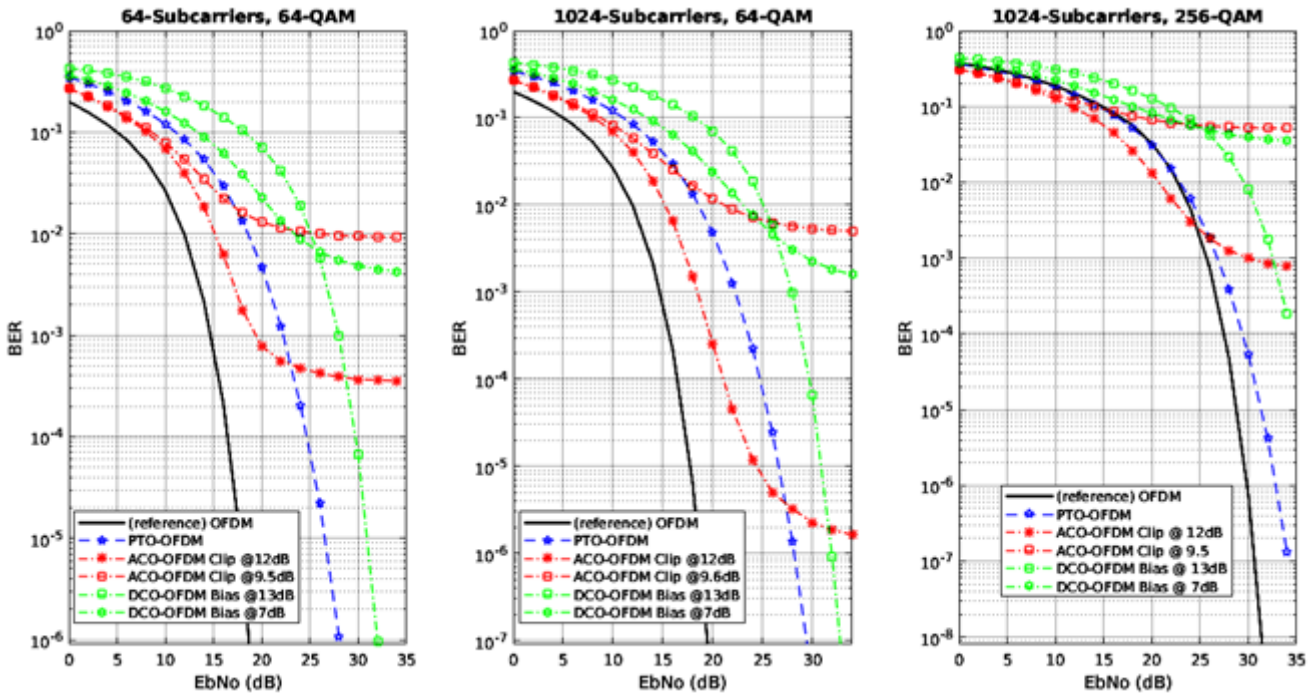

Fig. 10. PTO-OFDM vs Hermitian Symmetry OFDM

PTO model is contrasted with DCO-, ACO-OFDM regarding their BER. Hermitian Optical OFDM either floor at a given BER or performs behind PTO-OFDM as the energy per bit increases regardless of the clipping or biasing level employed

Fig. 10 gives a comparative result of both Hermitian and PTO-OFDM models. In addition to the improvement seen in link bandwidth efficiency that is, at least doubling of the data subcarriers effectiveness, PTO-OFDM preserves enhanced BER. Table 1 also shows data subcarriers usage of the optical OFDM and their respective frame length without considering the guard intervals and cyclic prefix.

The reach a practically significant BER, while increasing the SNR, the PTO-OFDM, has the advantage of maintaining and steady improving BER. On the other hand, depending on the bias level or the clip power, Hermitian optical OFDM tends toward BER floor. In the case of a DCO-OFDM bias at 7dB, the BER keeps improving as SNR increases but still not as the PTO [23]

V. CONCLUSION

A new polar based OFDM adapted to the VLC link is presented in this paper. It allows a simpler design of the transmit and receipt system by removing the need for a Hermitian symmetry transform as well as a DC biasing allowing more bandwidth and power for the valuable information signal. It addresses only the discrete model of system and processing. Significant improvement of the PAPR with minor BER deterioration is achieved at the cost of a modest augmentation of the OFDM subcarrier relative to the conventional OFDM setup.

Due to the difference in the nature of the angle and amplitude distribution, different quantization can be adopted to improve on the SQNR of the system. Besides, the lack of DC biasing would allow the use of power-efficient dimming, supported communication, which constitutes new areas to be investigated in future works.

REFERENCES

1. X. Guo, Y. Guo, and S. Li, "Experimental Investigation of Zadoff-Chu Matrix Precoding for Visible Light Communication System with OFDM Modulation," *Advances in Condensed Matter Physics*, 2018. https://www.hindawi.com/journals/acmp/2018/5173285/ (accessed Feb. 22, 2020).
2. F. Zafar, M. Bakaul, and R. Parthiban, "Laser-diode-based visible light communication: Toward gigabit class communication," *IEEE Communications Magazine*, vol. 55, no. 2, pp. 144–151, 2017.
3. N. Chi, Y. Zhou, S. Liang, F. Wang, J. Li, and Y. Wang, "Enabling technologies for high-speed visible light communication employing CAP modulation," *Journal of Lightwave Technology*, vol. 36, no. 2, pp. 510–518, 2018.
4. K. Bandara, P. Niroopan, and Y.-H. Chung, "PAPR reduced OFDM visible light communication using exponential nonlinear companding," in *2013 IEEE International Conference on Microwaves, Communications, Antennas and Electronic Systems (COMCAS 2013)*, Oct. 2013, pp. 1–5, doi: 10.1109/COMCAS.2013.6685269.
5. H. Elgala, S. K. Wilson, and T. D. Little, "Optical polar OFDM: On the effect of time-domain power allocation under power and dynamic-range constraints," in *IEEE Wireless Communications and Networking Conference (WCNC)*, New Orleans, LA, USA, Mar. 2015, pp. 31–35.
6. J. Lian and M. Brandt-Pearce, "Magnitude-Phase Optical OFDM for IM/DD Communication Systems," in *2018 52nd Asilomar Conference on Signals, Systems, and Computers*, 2018, pp. 702–706.
7. Z. Ghassemlooy, W. Popoola, and S. Rajbhandari, *Optical Wireless Communications: System and Channel Modelling with MATLAB®*, 1st ed. CRC Press, 2012.
8. S. B. Slimane, "Peak-to-average power ratio reduction of OFDM signals using broadband pulse shaping," in *Proceedings IEEE 56th Vehicular Technology Conference*, Sep. 2002, vol. 2, pp. 889–893 vol.2, doi: 10.1109/VETECF.2002.1040728.
9. Y. S. Cho, J. Kim, W. Y. Yang, and C. G. Kang, *MIMO-OFDM Wireless Communications with MATLAB*. John Wiley & Sons, 2010.
10. A. K. Gurung, F. S. Al-Qahtani, A. Z. Sadik, and Z. M. Hussain, "Power savings analysis of clipping and filtering method in OFDM systems," in *2008 Australasian Telecommunication Networks and Applications Conference*, 2008, pp. 204–208.
11. Xianbin Wang, T. T. Tjhung, and C. S. Ng, "Reduction of peak-to-average power ratio of OFDM system using a companding technique," *IEEE Transactions on Broadcasting*, vol. 45, no. 3, pp. 303–307, Sep. 1999, doi: 10.1109/11.796272.

12. S. Thompson, J. G. Proakis, and J. R. Zeidler, "The effectiveness of signal clipping for PAPR and total degradation reduction in OFDM systems," presented at the IEEE GLOBCOM, Jan. 2005, pp. 5 pp. – 2811, doi: 10.1109/GLOCOM.2005.1578271.
13. G. Sikri, "Peak to Average Power Ratio Reduction in OFDM System over PAM, QAM and QPSK Modulation," in *Advances in Computing and Information Technology*, Springer, 2012, pp. 685–690.
14. V. P. T. Ijyas and M. I. Al-Rayif, "Low Complexity Joint PAPR Reduction and Demodulation Technique for OFDM Systems," *IETE Journal of Research*, vol. 0, no. 0, pp. 1–11, Oct. 2019, doi: 10.1080/03772063.2019.1674194.
15. A. Skrzypczak, P. Siohan, and J.-P. Javaudin, "Analysis of the Peak-To-Average Power Ratio for OFDM/OQAM," in *2006 IEEE 7th Workshop on Signal Processing Advances in Wireless Communications*, Jul. 2006, pp. 1–5, doi: 10.1109/SPAWC.2006.346413.
16. S. Y. Le Goff, S. S. Al-Samahi, B. K. Khoo, C. C. Tsimenidis, and B. S. Sharif, "Selected mapping without side information for PAPR reduction in OFDM," *IEEE Transactions on Wireless Communications*, vol. 8, no. 7, pp. 3320–3325, Jul. 2009, doi: 10.1109/TWC.2009.070463.
17. H. Boche and B. Farrell, "On the peak-to-average power ratio reduction problem for orthogonal transmission schemes," *Internet Mathematics*, vol. 9, no. 2–3, pp. 265–296, 2013.
18. P. Varahram, W. A. Azzo, and B. M. Ali, "IDRG–PTS scheme with low complexity for peak-to-average power ratio reduction in OFDM systems," *Journal of the Chinese Institute of Engineers*, vol. 36, no. 6, pp. 677–683, Sep. 2013, doi: 10.1080/02533839.2012.740593.
19. S. B. Slimane, "Reducing the peak-to-average power ratio of OFDM signals through precoding," *IEEE Transactions on vehicular technology*, vol. 56, no. 2, pp. 686–695, 2007.
20. Y. Hong, X. Guan, L.-K. Chen, and J. Zhao, "Experimental demonstration of an OCT-based precoding scheme for visible light communications," in *2016 Optical Fiber Communications Conference and Exhibition (OFC)*, 2016, pp. 1–3.
21. L. Song and J. Shen, Evolved cellular network planning and optimization for UMTS and LTE. CRC press, 2010.
22. S. Bhattacharjee, M. Rakshit, S. Sil, and A. Chakrabarti, "Reduction of Peak-to-Average Power Ratio of OFDM System Using Triangular Distribution Based Modified Companding Scheme," *IETE Journal of Research*, vol. 64, no. 5, pp. 660–672, 2018.
23. J. Armstrong and B. J. Schmidt, "Comparison of asymmetrically clipped optical OFDM and DC-biased optical OFDM in AWGN," *IEEE Communications Letters*, vol. 12, no. 5, pp. 343–345, 2008.

AUTHORS PROFILE

Oumar Sacko received his BSc. degree in Telecommunication, department of Electronics and Electrical Engineering from Istanbul Technical University, Istanbul, Turkey, 2016. Presently, he is pursuing his MSc degree in Telecommunication in the Pan African University Institute of Basic Sciences Technology and Innovation hosted by Jomo Kenyatta University of Agriculture and Technology. Currently his research interest areas are visible light communications, wireless optical OFDM and PAPR reduction schemas for OFDM signals.

Stephen Musyoki graduated with a Bachelor of Engineering (B. Eng) from the University of Sierra Leone. He proceeded and did his Master of Engineering (M. Eng) at the University of Telecommunication in Tokyo and later did his Doctor of Engineering (D. Eng) at Tohoku University. After completing his D. Eng, he worked as a Research Fellow at the Japan Atomic Energy Research Institute (JAERI) for a period of two years. He was then employed as a Research and Development Engineer by NEC Corporation in Japan for a period of six years and later as an Engineer by Sangikyo Corporation in Japan for a period of two years. On returning to Kenya in 2003, he was employed as a Senior Lecturer at Jomo Kenyatta University of Agriculture and Technology (JKUAT) until 2014, and then joined the Technical University of Kenya (TUK) as an Associate Professor of Telecommunications and Information Engineering. He is currently the Director of the School of Electrical and Electronic Engineering in the same University.

Vitalice K. Oduol received his pre-university education at Alliance High School in Kenya. He was awarded a CIDA scholarship to study electrical engineering at McGill University, Montréal, Canada, where he received the B.Eng. (Hons.), M.Eng. and Ph.D. degrees in 1985,1987, and 1992, respectively, all in electrical engineering from McGill University. He was a research associate and teaching assistant while a graduate student at McGill University. He joined MPB Technologies, Inc. in 1989, where worked on meteor burst communication systems, satellite on-board processing, and low probability of intercept radio. In 1994 he joined INTELSAT where he did R&D work on the integration of terrestrial wireless and satellite systems. After working at COMSAT Labs. (1996-1997) on VSAT networks, and TranSwitch Corp.(1998-2002) on communication systems product definition and architecture, he returned to Kenya, where since 2003 he has been with Department of Electrical and Information Engineering, University of Nairobi. From 2006 to 2012 he was chairman, Department of Electrical and Information Engineering, University of Nairobi. His research interests include performance of communication systems – analysis, modeling, simulation and evaluation. This includes signal processing, spectrum Sensing in Cognitive Radio, emerging areas (5G and beyond), Mitigation of Rain attenuation in RF signals at high frequencies. He is also interested in vehicle-to-vehicle V2V) communications, vehicle-to-infrastructure (V2I) communications. Prof. Oduol is a member of IEEE, and was a two-time recipient of the Douglas Tutorial Scholarship at McGill University.